Theoretical Study of Aluminum-Sodium Bimetallic Clusters. I. Geometrical and Electronic Structures of Al_nNa (n=1—4)

Hidenori MATSUZAWA,† Toshiyuki HANAWA, Kazunori SUZUKI, and Suehiro IWATA*
Department of Chemistry, Faculty of Science and Technology, Keio University, Hiyoshi, Kohoku-ku, Yokohama 223
(Received May 12, 1992)

The geometrical and electronic structures of several small aluminum-sodium mixed clusters Al_nNa and pure aluminum clusters Al_n (n=1—4) were examined with ab initio MO calculations. All the calculations were carried out at the restricted Hartree–Fock level of approximation for both closed and open shell systems. The structures of the most stable Al_n cluster and neutral and cationic Al_nNa clusters were fully optimized. The low and high spin multiplicities of each cluster were examined. The structure of the most stable state of the Al_nNa clusters keeps the frame of the Al cluster unchanged, and the Al–Al distances become shorter than in the corresponding Al clusters. The calculated ionization energies by the ΔSCF method are qualitatively in agreement with the corresponding experimental values. The highest occupied molecular orbital of the neutral clusters suggests that an ionized electron is localized on the Al atoms, but the large orbital reorganization by ionization results in a substantial net positive charge on a sodium atom. The nature of chemical bond for the clusters is also examined.

Recently, many experimental studies of the metallic clusters have been reported with the development of the molecular beam technique, high sensitive laser spectroscopy and high-resolution time-of-flight mass-spectroscopy. The detailed study on the metallic cluster plays an important role in understanding the change of chemical bonds from the covalent bond to the metallic bond. The metallic cluster is expected to have the properties of both molecules and metals. In particular, the bimetallic cluster is noted as a new catalysis and a new material. It is known that the alkali metal adsorbed on transition metal surface reduces the work function and plays a role as a promoter in catalysis.[1,2] The substantial numbers of papers are devoted to studying their chemical properties and electronic structures both experimentally and theoretically. In the experimental studies of the pure alkali metal clusters, the cluster size dependence of the stability, of the ionization energy and of the other properties is reported.[3] Some of the characteristics of the alkali metal clusters are well explained by the shell model, theoretically. Also the systematic studies with ab initio SCF MO (CI) methods are reported.[4]

The bimetallic clusters are also examined as well as the pure metallic clusters, experimentally. It is important to study the effects of the heteloatom on the chemical properties, stability and reactivity in the mixed cluster. Nakajima, Hoshino, Naganuma, Sone and Kaya[5] in our department have reported the ionization energy and the reactivity to a hydrogen molecule of the aluminum–sodium bimetallic clusters (Al_nNa_m). They have shown that the ionization energy (I_p) decreases with the number of sodium atoms, m. They also found the systematic decrease of I_p of Al_nNa by 0.2—0.6 eV from I_p of the corresponding Al_n cluster except at n=13 and n=23; I_p of $Al_{13}Na$ and $Al_{23}Na$ are slightly higher or equal to I_p of the corresponding pure clusters.

The aim of this work is to explore the experimental results and to get some information which is not obtained directly from the experimental study. The mixed clusters Al_nNa_m (n=1—4, m=1; n=1—3, m=2; n=1—2, m=3) are examined with the ab initio SCF MO calculations. In this paper the optimized geometry and electronic structure of the Al_nNa clusters are mostly discussed. In the subsequent paper[6] we report the results of the clusters having more than one sodium atoms ($m\geq 2$). Before the geometry optimization of the Al_nNa clusters, the geometries of the Al_n (n=1—4) clusters are optimized and compared with those of the more extensive Pettersson and Bauschlicher's results which includes the Davidson correction (CCI+Q)[7] and with those of Upton's GVB calculations.[8]

Calculations

The geometrical and electronic structures of the Al clusters (Al_2, Al_3, and Al_4), Al_nNa clusters (AlNa, Al_2Na, Al_3Na, and Al_4Na), their cationic clusters ($AlNa^+$, Al_2Na^+, Al_3Na^+, and Al_4Na^+) and their component atoms (Al and Na) were studied with the ab initio restricted Hartree–Fock wavefunctions (RHF) for both closed and open shell clusters. The geometry of all clusters was optimized by using the analytical energy gradient method. After the geometry optimization of the neutral Al_nNa clusters, the geometry of their cationic clusters was optimized by starting from the equilibrium geometry of the neutral clusters. The stability of the mixed clusters, except for several Al_4Na^+ clusters, was examined by evaluating the harmonic frequencies. The basis set used was 6—31G. The computer programs used were GAMESS (NDSU version),[9] GAMESS (IMS version)[10] and GAUSSIAN 88[11] program packages. All calculations were performed with KUBOTA

† Present address: Department of Chemistry, Faculty of Science, Rikkyo University, Nishi-ikebukuro, Toshima-ku, Tokyo 171.

MIPS 3330 engineering workstation in our laboratory and with HITAC S-820 at the Institute for Molecular Science (IMS).

In the preminary geometry optimization of all the possible structure in linear Al_2Na, $AlNa_2$, and Al_2Na_2 clusters, it was found that the Al_2 frame was kept unchanged but the Na_2 frame is broken: the Al–Na–Al, Na–Na–Al, and Al–Na–Na–Al structures are unstable, and Al–Al–Na, Na–Al–Na, and Na–Al–Al–Na structures are stable. Thus, to determine the stable geometry of Al_nNa clusters, we assumed that the bimetallic cluster was a aluminum cluster Al_n adsorbed by a sodium atom Na. Therefore, the geometry optimization of the neutral cluster Al_n (n=2—4) was first carried out. Pettersson and Bauschlicher,[7] and Upton[8] already reported the structure and the multiplicity of several Al_n clusters with the correlated wavefunction. Thus, by comparing our results with theirs, we could assess our approximation. To optimize the geometry of Al_nNa, we examined most of possible approaches of a Na atom to the Al_n clusters; for instance, to the end atom, to the middle of the bond, and in-plane and out-of-plane approaches. The symmetry was first assumed to be C_1, and then under the possible high symmetry found in the preliminary calculations, the geometry of each cluster was re-optimized.

All the geometries of the cationic (Al_nNa^+) (n=1—4) clusters were also optimized. The initial geometry was the equilibrium structure of the corresponding neutral clusters.

The vertical ionization energy of the Al_nNa clusters was estimated at the optimized neutral structure. The atomization energy per atom was evaluated by using the equation proposed by Pewestorf et al.[12]

$$E_b/(n+1)=(nE_{Al}+E_{Na}-E_n)/(n+1),$$

where E_n is the energy of the Al_nNa cluster, and E_{Al} and E_{Na} are the energy of an Al atom and a Na atom, respectively.

Before discussing the calculational results, we should mention the approximation we applied. The electrons in aluminum and sodium clusters are delocalized within the clusters, and the dynamical screening of the electrostatic potentials between the ion cores and the electron as well as between the electron and the electron is so efficiently operative; thus the free-electron-like theories such as a jerrium model and a shell model do apparently work effectively. In the teminolgy of the molecular orbital theory, it implies that the dynamical electronic correlation is very important in the electron wavefunction of the clusters. In the present work, we restrict ourselves to the use of the restricted Hartree–Fock wavefunction. By knowing the limitation of the approximation, we have to assess the present results with care. In particular, it is true when the energy of the states with different spin multiplicities is compared, because the approximation is better for the state with higher multiplicity than for the state with lower multiplicity. In the following section we will see repeatedly that the triplet (quartet) state is more stable than the singlet (doublet) state in the even (odd) electron system in the RHF approximation.

Results and Discussion

Geometry Optimization of the Al Clusters. The optimized geometrical parameters and the atomization energy of the Al clusters, Al_2, Al_3, and Al_4, are listed in Table 1 with the corresponding Pettersson and Bauschlicher's CCI+Q results.[7]

There are two possible low-lying valence electronic configurations in diatomic Al_2 molecule,

$$Al(^2\Pi)+Al(^2\Pi)\rightarrow {}^3\Pi_u(1\sigma_g)^2(1\sigma_u)^2(2\sigma_g)^1(1\pi_u)^1$$
$$ {}^3\Sigma_g^-(1\sigma_g)^2(1\sigma_u)^2(1\pi_{u+})^1(1\pi_{u-})^1.$$

The ground state is the $^3\Pi_u$ state, which agrees with Pettersson and Bauschlicher's CCI+Q calculation. Hereafter, we number the molecular orbitals excluding the core orbitals for simplicity. The experimental results with the molecular beam technique also support the ground $^3\Pi_u$ state of Al_2.[13] On the contrary, the ground state of the isovalent diatomic molecule B_2 is $^3\Sigma_g^-$.[14] The dissociation energy, D_e, of the $^3\Pi_u$ state at the SCF level (0.51 eV) is smaller than that at CCI+Q

Table 1. Geometrical Parameters and Dissociation Energy D_e of Al Clusters

			RHF/6—31G			CCI+Q/ECP[a]		
			R_e/Å[b]	D_e/eV	D_e/atom/eV	R_e/Å	D_e/eV	D_e/atom/eV
Al_2	$^3\Pi_u$	($D_{\infty h}$)	2.83	0.51	0.25	2.75	1.20	0.60
	$^3\Sigma_g^-$		2.65	0.12	0.06	2.52	1.10	0.55
Al_3	$^4A_2$	(C_{2v})	2.75/76.2[c]	1.28	0.43	2.62/71.0	2.75	0.92
	$^2A_1$		2.69/61.7	0.53	0.18			
	$^2A_1'$	(D_{3h})	2.72	0.53	0.18	2.59	2.74	0.92
	$^2A_2''$		2.85	0.49	0.16	2.86	2.63	0.88
	$^4\Sigma_u^-$	($D_{\infty h}$)	2.66	1.17	0.39	2.62	2.34	0.78
Al_4	$^3B_{1u}$	(D_{2h})	2.97	1.41	0.35	2.67	4.35	1.09

a) Ref. 7. b) The R_e is the Al–Al equilibrium distance. c) Given as R_e/angle (deg.).

level (1.20 eV). The difference between a $^3\Pi_u$ and a $^3\Sigma_g^-$ state in the dissociation energy, D_e, is 0.39 eV, which is larger than the CCI+Q calculation (0.10 eV), but agrees with the SCF calculations (0.36 with DZ and 0.39 eV with TZ) by Pettersson and Bauschlicher.[15] The Al–Al bond distance of the ground state is 2.830 Å, which is a little longer than that of the CCI+Q level, 2.751 Å, and agrees again with the SCF level with DZ and TZ; 2.899 (DZ) and 2.868 Å (TZ). Both CCI+Q and SCF calculations fail to reproduce the experimental equilibrium bond distance 2.701 Å.[16] The Al–Al distance of the $^3\Sigma_g^-$ state is shorter than that of the ground state. It suggests that the π orbital contributes to forming the Al–Al bonding more than the σ orbital.

The most stable conformation of trimer Al_3 in our calculations is in a triangular form,

$$^4A_2[(1a_1)^2(2a_1)^2(1b_2)^2(1b_1[\pi])^1(3a_1)^1(2b_2)^1]\ (C_{2v})$$

as in Pettersson and Bauschlicher's paper.[7] Upton[8] reported that the ground state is $^2A_1$ and that the $^4A_2$ state is the excited state in his GVB and CI calculations. In our calculation

$$^2A_1[(1a_1)^2(2a_1)^2(1b_2)^2(1b_1[\pi])^2(3a_1)^1]\ (C_{2v})$$

lies higher than the $^4A_2$ state. Pettersson and Bauschlicher did not study the $^2A_1$ state. In addition to C_{2v} conformers, we have located the stationary structure at D_{3h},

$$^2A_1'[(1a_1')^2(1e')^4(1a_2''[\pi])^2(2a_1')^1]$$

and

$$^2A_2''[(1a_1')^2(1e')^4(2a_1')^2(1a_2''[\pi])^1],$$

as did Pettersson and Bauschlicher. In our calculation the deformation energy from D_{3h} to C_{2v} is only 0.005 eV.

We have also located a stable linear structure

$$^4\Sigma_u^-[(1\sigma_g)^2(2\sigma_g)^2(1\sigma_u)^2(2\sigma_u)^1(1\pi_{u+})^1(1\pi_{u-})^1]\ (D_{\infty h}).$$

In the RHF approximation, the dissociation energy of the triplet state is about a half of CCI+Q value, while for the singlet state it is a fifth. Very recently the ESR spectrum of Al_3 isolated in Ar matrix is reported.[17] The spectrum indicates that the trimer is the doublet state, and three atoms are magnetically equivalent. But, this does not means that the ground state is $^2A_1'$ or $^2A_2''$ having D_{3h} symmetry. Because the deformation energy to a C_{2v} conformer is very small and less than thermal energy, the ESR spectrum of three equivalent aluminum atoms might be observed, even if the most stable conformer is at C_{2v}.

Pettersson and Bauschlicher reported[7] that the most stable state of Al_4 cluster is the $^3B_{1u}$ state $[(1a_g)^2(1b_{1u})^2(1b_{2u})^2(2a_g)^2(1b_{3g})^2(3a_g)^1(2b_{1u})^1]$ of the rhombus D_{2h} symmetry, while in the calculations by Upton[8] the $^1A_1$ state of the non-planar C_{2v} symmetry is most stable at the dihedral angle of 151.7° around the shorter Al–Al axis. In our calculation the rhombus $^3B_{1u}$ state

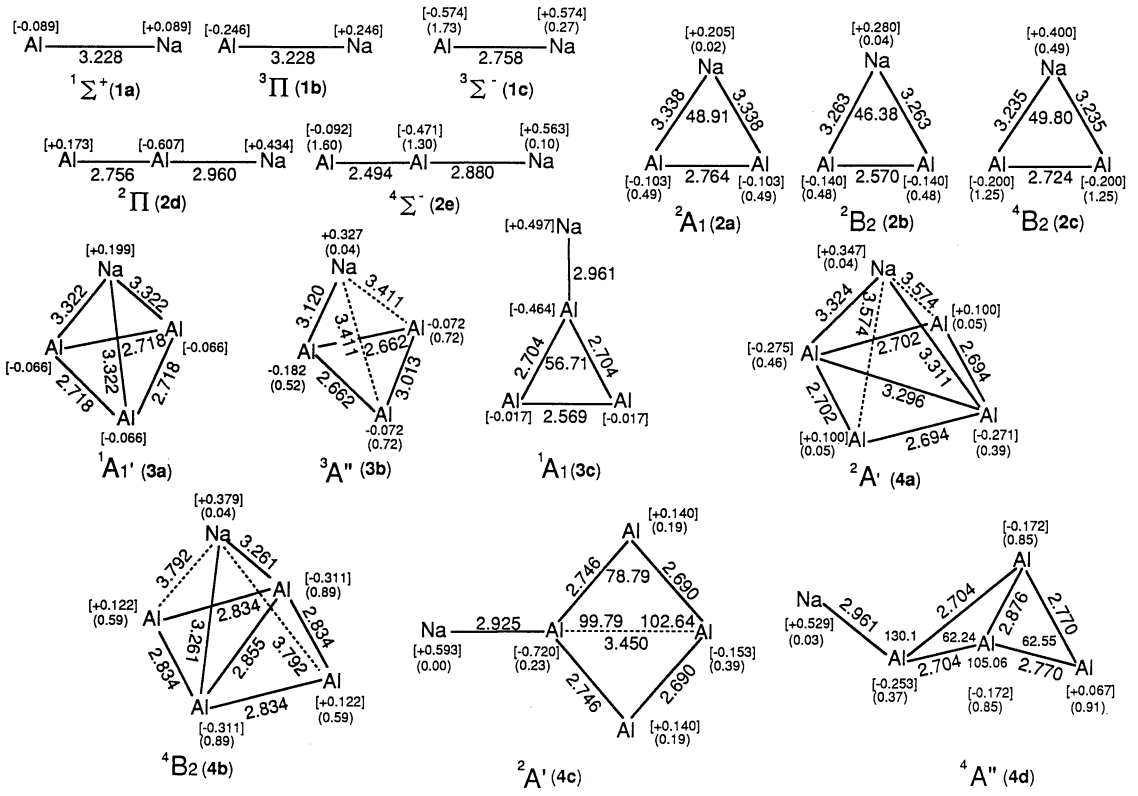

Fig. 1. Optimized geometries of the neutral Al_nNa (n=1—4) cluster. Where the Mulliken gross population in square brackets and the spin density in parentheses are also given.

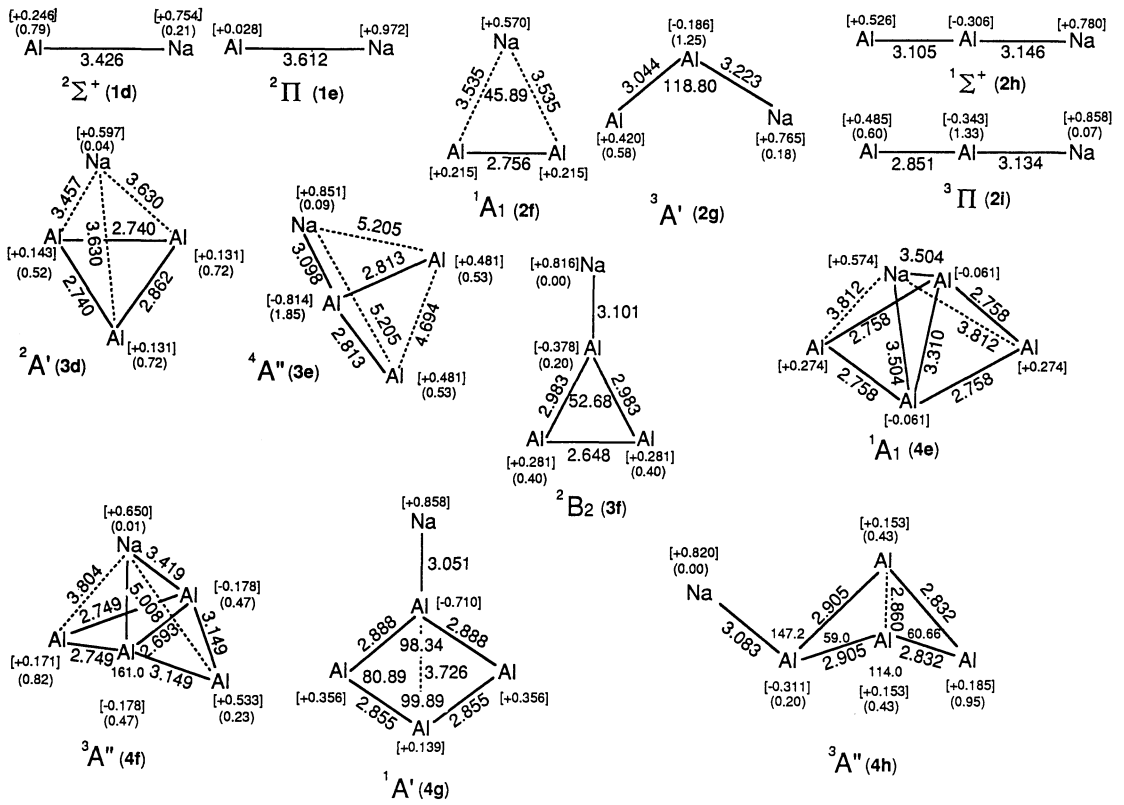

Fig. 2. Optimized geometries of the cationic Al_nNa^+ (n=1—4) cluster. Where the Mulliken gross population in square brackets and the spin density in parentheses are also given.

is most stable. The shortest Al–Al bond distance of this state is 2.752 Å in our calculation, which is longer than the CCI+Q value of 2.619 Å. The atomization energy of the SCF level with 6—31 G is about a half of the CCI+Q level.

The comparison of the present calculations for the pure aluminum clusters with the other calculations suggests that the Al–Al distance in the RHF calculation tends to be longer by 0.1 Å than in CCI+Q approximation and that the energy gap between the higher and lower multiplicities is larger in the RHF approximation than in CCI+Q and GVB approximations because of the poor approximation to the lower multiplicity in the former.

Geometries of the Neutral and Cationic AlNa Clusters. The optimized geometries of the neutral and cationic Al_nNa (n=1—4) clusters are shown in Figs. 1 and 2, respectively, where the Mulliken gross population in square brackets and the spin density in parentheses are also given. For each cluster, all of local minimal geometries located are shown in the figure. The relative energy from the most stable state, T_e, and the stabilization energy from Al_n (n=1—4) and a Na, ΔE_{Al_n+Na}, and the atomization energy, $E_b/(n+1)$ in Eq. 1 are listed in Table 2. The relative energy, T_e, and $\Delta E_{Al_n+Na^+}$, of the cation clusters are listed in Table 3.

Three electronic states, $^1\Sigma^+[(1\sigma)^2(2\sigma)^2]$ (**1a**), $^3\Pi[(1\sigma)^2(2\sigma)^1(1\pi)^1]$ (**1b**), and $^3\Sigma^-[(1\sigma)^2(1\pi_+)^1(1\pi_-)^1]$ (**1c**), of the neutral diatomic AlNa molecule have a minimum in their potential energy curves with the RHF calculations. Hereafter, each state of Al_nNa is labeled as (**na**) in text, figures and tables. For comparison we have carried out the multi-reference single and double (MRSD) CI calculations with triple zeta+polarization of quality.[18] The above three states are also bound in the CI potential energy curves; the ground state is $^1\Sigma^+$ with R_e=3.181 Å. On the contrary to the CI results, in the RHF approximation the $^3\Pi$ state is lower than the $^1\Sigma^+$ state by 0.22 eV. This is another example that the RHF wavefunction for the high multiplicity is again better than for the closed shell state. Because of the poor approximation of the RHF wavefunction to the closed shell metal diatomic molecule, the ΔE_{Al_n+Na} of the closed shell ground state $^1\Sigma^+$ is higher (by 0.118 eV) than the sum of the total energy of Al(^{2}P) and Na(^{2}S). This phenomena are occasionally found for some of weak diatomic molecules. In our MRSD CI calculations with a large basis set the dissociation energy of the $X^1\Sigma^+$ is 0.71 eV, which is still about a half of the thermochemically estimated value (1.40 eV). The $^3\Sigma^-$ state is also bound, but the energy of this state is higher (by 0.891 eV) than that of the lowest triplet state. The calculated equilibrium bond distance R_e of both the $^1\Sigma^+$ state and the $^3\Pi$ state is 3.228 Å and R_e of the $^3\Sigma^-$ state is 2.758 Å. Since the experimental R_e is not known, the R_e's at the RHF calculations are compared with our SD CI calculation results. The R_e for $X^1\Sigma^+$ is 3.181 Å, R_e for $^3\Pi$ is 3.021 Å and R_e for $^3\Sigma^-$ is 2.731 Å at the SD CI level. The R_e

Table 2. Stabilization and Atomization Energies of Al_nNa Clusters

		State	T_e/eV[a]	D_e/eV[b]	$E_b/(n+1)$/eV[c]	ΔE_{Al_n+Na}/eV[d]
AlNa	($C_{\infty v}$)	$^1\Sigma^+$ **(1a)**	0.224	−0.118	−0.059	−0.118
		$^3\Pi$ **(1b)**	0.000	0.106	0.053	0.106
		$^3\Sigma^-$ **(1c)**	0.891	−0.785	−0.393	−0.785
MRSD-CI		$^1\Sigma^+$	0.000	0.705	0.353	
		$^3\Pi$	0.250	0.477	0.239	
		$^3\Sigma^-$	1.118	1.795	0.898	
Al_2Na (Triangular)	(C_{2v})	$^2A_1$ **(2a)**	0.235	0.760	0.253	0.252
		$^2B_2$ **(2b)**	0.471	0.524	0.175	0.016
		$^4B_2$ **(2c)**	0.000	0.995	0.332	0.487
(Linear)	($C_{\infty v}$)	$^2\Pi$ **(2d)**	0.283	0.712	0.237	0.204
		$^4\Sigma^-$ **(2e)**	0.076	0.919	0.306	0.411
Al_3Na (Tetrahedral)	(C_{3v})	$^1A_1'$ **(3a)**	0.431	1.454	0.364	0.178
	(C_s)	$^3A''$ **(3b)**	0.000	1.886	0.472	0.609
(Vertex)	(C_{2v})	$^1A_1$ **(3c)**	0.670	1.216	0.304	−0.239
		$^3B_{2(TS)}$[e]	0.281	1.605	0.401	0.328
		$^3A_{1(TS)}$	0.998	0.888	0.222	−0.388
(Side)	(C_{2v})	$^1A_{1(TS)}$	0.826	1.060	0.265	−0.217
		$^3A_{2(TS)}$	0.734	1.152	0.288	−0.125
		$^3B_{1(TS)}$	0.756	1.130	0.283	−0.147
Al_4Na (Pentahedral)	(C_{2v})	$^2A_{1(TS)}$	0.362	2.519	0.504	1.106
	(C_s)	$^2A'$ **(4a)**	0.362	2.519	0.504	1.106
	(C_{2v})	$^4B_2$ **(4b)**	0.000	2.882	0.576	1.468
(Vertex)	(C_s)	$^2A'$ **(4c)**	0.572	2.310	0.462	0.897
		$^4A''$ **(4d)**	0.423	2.459	0.492	1.045

a) The term energy, T_e shows the relative energy from the most stable state. b) The D_e is the dissociation energy to the component atoms. c) The $E_b/(n+1)$ means the atomization energy per atom. d) The ΔE_{Al_n+Na} is the adsorption energy of the Na atom on the Al_n cluster. The plus means stable, and the minus means unstable. e) The TS shows that this stationary point is the transition state.

Table 3. Relative Energies from Most Stable State and the Adsorption Energies of a Na^+ on the Al_n (n=1—4) Clusters in the Al_nNa^+ Clusters

		State	T_e/eV[a]	$\Delta E_{Al_n+Na^+}$/eV[b]
$AlNa^+$	($C_{\infty v}$)	$^2\Sigma^+$ **(1d)**	0.000	0.794
		$^2\Pi$ **(1e)**	0.788	0.006
MRSD-CI		$^2\Sigma^+$	0.000	
		$^2\Pi$	0.634	
Al_2Na^+ (Triangular)	(C_{2v})	$^1A_1$ **(2f)**	0.838	0.220
	(C_s)	$^3A'$ **(2g)**	0.134	0.924
	(C_{2v})	$^3A_{1[TS]}$	0.319	0.739
(Linear)	($C_{\infty v}$)	$^1\Sigma^+$ **(2h)**	0.000	1.058
		$^3\Pi$ **(2i)**	0.192	0.866
Al_3Na^+ (Tetrahedral)	(C_s)	$^2A'$ **(3d)**	0.640	0.478
		$^4A''$ **(3e)**	0.000	1.118
(Vertex)	(C_{2v})	$^2B_2$ **(3f)**	0.486	0.632
Al_4Na^+ (Pentahedral)	(C_{2v})	$^1A_1$ **(4e)**	0.351	0.939
	(C_s)	$^3A''$ **(4f)**	0.000	1.290
	(C_{2v})	$^3B_{2[TS]}$	0.014	1.276
(Vertex)	(C_s)	$^1A'$ **(4g)**	0.076	1.214
		$^3A''$ **(4h)**	0.019	1.271

a) The T_s is the relative energy from the most stable state. b) The $\Delta E_{Al_n+Na^+}$ is the adsorption energy of the Na^+ on the Al_n cluster.

of the $^3\Sigma^-$ state is shorter than that of the $^1\Sigma^+$ and $^3\Pi$ state in both calculations. It suggests that the orbital 1π contributes to the Al–Na bonding more than the orbital 2σ which has also a bonding character. As is shown at the top of Fig. 1, in the SCF wavefunction of the closed shell $^1\Sigma^+$ state, the Al–Na bond is weakly covalent; no charge transfer from a Na atom to an Al atom takes place. On the other hand, in the RHF wavefunction of the $^3\Pi$ and $^3\Sigma^-$ states, the charge-transfer from $3s_{Na}$ of Na to $3p\sigma_{Z_{Al}}$ of Al and the back-charge-transfer from $3p\pi_{Al}$ to $3p\pi_{Na}$ of Na play an important role in bonding.

The ground state of the cation $AlNa^+$ is $^2\Sigma^+$ $[(1\sigma)^2(2\sigma)^1]$ (**1d**); the bond length with the RHF wavefunction is longer than that of the AlNa ground state $^1\Sigma^+$, which suggests that the orbital 2σ, mostly consisting of $3s_{Na}$ and $3p\sigma_{Z_{Na}}$, is, in fact, of bonding nature. The positive charge is mostly localized on Na, but it does not mean that the highest occupied molecular orbital (HOMO) 2σ of AlNa is $3s_{Na}$; in the canonical orbital set HOMO has substantially large coefficients on $3p\sigma_{Z_{Al}}$. The energy of $^2\Pi$ $[(1\sigma)^2(1\pi)^1]$ (**1e**) state is very high. The bond length of this state is longer than that of the $^3\Sigma^-$ state, which again suggests that the orbital 1π, mostly consisting of $3p\pi_{Al}$, contributes to the Al–Na bond.

Geometries of the Neutral and cationic Al_2Na Clusters. To optimize the geometry of Al_2Na, two approaches of a Na atom to Al_2, perpendicular to the molecular axis and colinear, are examined. Because two electronic states, $^3\Pi_u$ and $^3\Sigma_g^-$of Al_2 lie closely to each other, correspondingly the mixed triatomic Al_2Na has the isomers and low-lying states. We have located a C_{2v} isomer and a $C_{\infty v}$ isomer. The parentage of the following Al_2Na isomers is Al_2 ($^3\Pi_u$) as

$Al_2[^3\Pi_u; (1\sigma_g)^2(1\sigma_u)^2(2\sigma_g)^1(1\pi_u)^1] + Na\ (^2S)$
$\rightarrow {}^2A_1[(1a_1)^2(1b_1)^2(2a_1)^2(3a_1)^1]$ (C_{2v}) (**2a**),
$^2B_2[(1a_1)^2(1b_1)^2(2a_1)^2(1b_2[\pi])^1]$ (C_{2v}) (**2b**),
$^4B_2[(1a_1)^2(1b_1)^2(2a_1)^1(3a_1)^1(1b_2[\pi])^1]$ (C_{2v}) (**2c**),
$^2\Pi[(1\sigma)^2(2\sigma)^2(3\sigma)^2(1\pi)^1]$ ($C_{\infty v}$) (**2d**),

and the parentage of a linear $C_{\infty v}$ isomer is Al_2 ($^3\Sigma_g^-$) as

$Al_2[^3\Sigma_g^-; (1\sigma_g)^2(1\sigma_u)^2(1\pi_{u+})^1(1\pi_{u-})^1] + Na\ (^2S)$
$\rightarrow {}^4\Sigma^-\ [(1\sigma)^2(2\sigma)^2(3\sigma)^1(1\pi+)^1(1\pi-)^1]$ ($C_{\infty v}$) (**2e**).

The most stable state in our calculations is the triangular $^4B_2$ state (**2c**). The other states examined are also at a local minimum of the neutral Al_2Na, because all the calculated harmonic frequencies are real. The next stable state is the linear $^4\Sigma^-$ state which lies close to the $^4B_2$ state; the energy difference is 0.076 eV. The linear $^4\Sigma^-$ state is a precursor to the linear Al_2Na_2, which is the most stable among the isomers.[6] The bond distance Al–Al, $R_{Al\text{-}Al}$, in the triangular $^4B_2$ state is shorter by 0.11 Å than that in Al_2. This shrinkage of the Al–Al distance is the general characteristics in the mixed clusters as will be seen more in the subsequent subsections. The shortening is more dramatic in the linear $^4\Sigma^-$ state and the triangular $^2B_2$ state. In the triangular form (C_{2v}), the orbital $2a_1$ is the bonding orbital between the in-plane component of $1\pi_u$ of Al_2 and s and p orbitals of Na, and the orbital $3a_1$ is mostly of $2\sigma_g$ of Al_2. The orbital $1b_2$ is the out-of-plane component of $1\pi_u$ of Al_2.

The shorter $R_{Al\text{-}Al}$ in the $^2B_2$ state (**2b**) suggests that the orbital $2a_1$ contributes the shortening of $R_{Al\text{-}Al}$. In the $^2A_1$ state (**2a**), $R_{Al\text{-}Al}$ is shorter than that of $Al_2(^3\Pi_u)$ and longer than that of the $^2B_2$ state of Al_2Na. It suggests that the orbital $1b_2$ contributes to the bonding of Al_2 more than the orbital $3a_1$. The bond distance

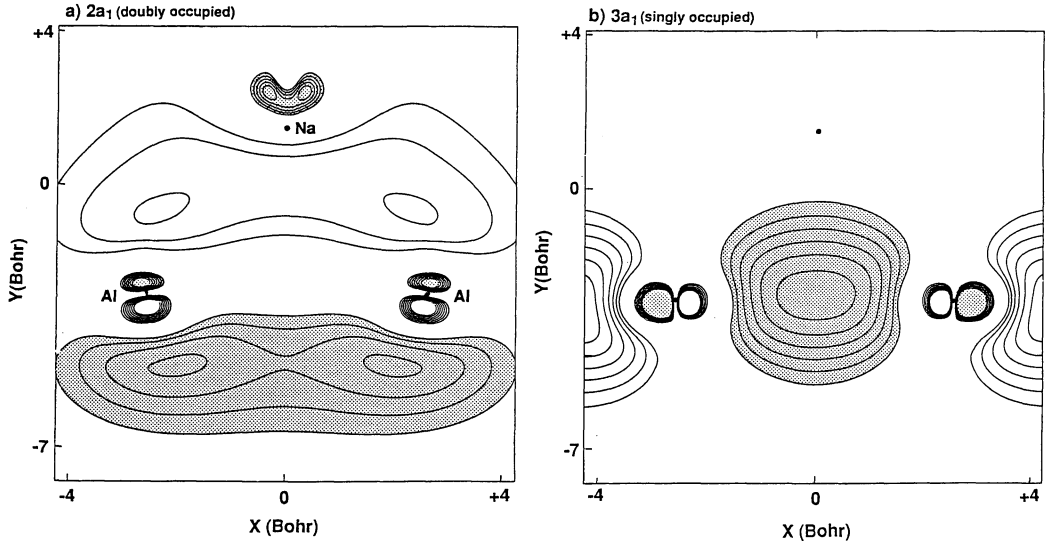

Fig. 3. Molecular orbitals contour maps at SCF level with DZ quality, a) orbital $2a_1$ and b) orbital $3a_1$, of $^2A_1$ state (Al_2Na). The shaded parts are negative phase. The positive contour lines are 0.03, 0.04, ..., 0.10 and the negative contour lines are −0.03, −0.04, ..., −0.10 bohr^3.

R_{Al-Na} in the triangle form is nearly equal to that of the diatomic AlNa. On the other hand, in the linear form $^4\Sigma^-$, both bond distances become shorter than the corresponding diatomic molecule. Because a pair of the singly occupied 1π orbital is mostly localized on Al_2, the small spin density (0.1) on Na implies that the orbital 3σ is also the orbital on Al_2, which suggests that unoccupied $2\sigma_g$ of Al_2 becomes 3σ in the linear Al_2Na. This explains the shortening of R_{Al-Al}. In the $^2\Pi$ state, R_{Al-Al} is also shorter than that of the diatomic molecule because the orbital 3σ becomes doubly occupied. From the comparison with R_{Al-Al} of the $^4\Sigma^-$ state, it is suggested again that the orbital 1π contributes to the shortening of R_{Al-Al}. By knowing the general trend of the poorer approximation for the lower spin multiplicity, the most probable true ground state is the doublet state, either $^2A_1(C_{2v})$ or $^2\Pi(C_{\infty v})$.

The contour maps of the orbitals of $^2A_1$ (**2a**) are shown in Fig. 3. The figure suggests that the Al–Na bond is formed between the π orbital of Al_2 and the $3p_z$ of Na, though the molecular orbital coefficients of s type basis set on the Na atom is larger than those of $3p_z$ type. As the net charge on a Na atom is small (+0.21), the bond is not much ionic. The Al–Na bond in the Al_2Na seems to be the three-center two-electron bond as in diborane. One of findings in the present study is that the Al–Al bond is shortened by the Na adsorption. In Al_2Na the orbital $2a_1$, which forms the three-center two-electron bond, also contributes to strengthening the Al–Al bond. The orbital $3a_1$ (Fig. 3b), which is SOMO, forms only the Al–Al σ bond. Figure 3b clearly shows that an electron of the orbital $3a_1$ localized on Al_2.

Starting from the stable geometry of the neutral Al_2Na, we determined the triangle and linear cation Al_2Na^+. The closed shell $^1\Sigma^+$ $[(1\sigma)^2(2\sigma)^2(3\sigma)^2]$ (**2h**) is the lowest state among the linear and triangular isomers. Because, as is already discussed, the RHF calculation tends to favor the higher multiplicity, the linear $^1\Sigma^+$ is most likely the ground state of Al_2Na^+. This state is generated by a removal of an electron from the orbital 1π of the $^2\Pi$ state, and is also correlated with the $^1A_1$ (**2f**) state of C_{2v}, which is generated by a removal of an electron either from the orbital $3a_1$ of $^2A_1$ (**2a**) or from the orbital $1b_2$ of $^2B_2$ (**2b**). By the harmonic frequency analysis the state (**2f**) is confirmed to be at the local minimum on the singlet surface. The Al–Al and Al–Na distances of the $^1\Sigma^+$ state is longer than that of the neutral $^2\Pi$ state because an electron is removed from the orbital 1π, which contributes to the shortening of R_{Al-Al}. The charge on Na increases by +0.35 with the ionization; the large orbital reorganization within the σ orbitals are responsible, because the ionized orbital is the 1π orbital mostly localized on Al_2 in the neutral cluster $^2\Pi$.

The removal of an electron from $2a_1$ of $^2A_1(C_{2v})$ or from $1b_2[\pi]$ of $^4B_2(C_{2v})$ leads to the triplet state $^3A'$ (**2g**) of C_s symmetry. At their vertical ionized geometry, an imaginary harmonic frequency, $84.09i$ cm^{-1} is found for the asymmetric motion. The symmetry of C_{2v} in the triangular triplet Al_2Na^+ is broken to C_s, and the $^3A_1$ state, which is now the transition state, becomes the $^3A'$ state; the singly occupied orbital $2a_1$ and $3a_1$ becomes the orbital 3a′ and 4a′, respectively. The triplet state $^3A'$ is at the local minimum because all the harmonic frequencies are real. The charge on Na increases by 0.46 in the $^3A'$ state when an electron is removed from the orbital $2a_1$ ($1b_2[\pi]$).

The linear triplet state $^3\Pi$ $[(1\sigma)^2(2\sigma)^2(3\sigma)^1(1\pi)^1]$ (**2i**) is formed by the ionization of $^4\Sigma^-$ state. The Al–Al distance, R_{Al-Al} of this state is longer than that of the $^4\Sigma^-$ state and shorter than that of $^1\Sigma^+$ state.

Geometries of the Neutral and Cationic Al_3Na Clusters. Because the most stable structure of Al_3 is a triangle form of $^4A_2$ and $^2A_1'$, we examined the triangle Al_3 cluster adsorbed by a Na atom. The linear Al_3 attached by a Na atom is not discussed in present subsection, though the linear Al_3 is also stable. There are two ways how a Na atom approaches to the Al_3 cluster; one is out-of-plane, and the other is in-plane. In the in-plane approach, the side and vertex approaches are possible. In each of three approaches we have located the stationary geometry on the potential energy surfaces of both singlet and triplet states. The real stability on each surface is confirmed by examining the eigenvalues of the force constant matrix at the stationary geometry.

The most stable triplet state of the mixed cluster Al_3Na in the RHF approximation is the $^3A''$ state (**3b**) of a distorted tetrahedral form with C_s symmetry. This cluster is formed from $^4A_2[(1a_1)^2(2a_1)^2(1b_2)^2(1b_1[\pi])^1(3a_1)^1(2b_2)^1]$ of the Al_3 cluster. The electron configuration is

$$^3A''[(1a')^2(1a'')^2(2a')^2(3a')^2(4a')^1(2a'')^1]\ (C_s)\ (\mathbf{3b}).$$

The parentage of the singly occupied molecular orbitals (SOMO) 2a″ and 4a′ is the orbitals $2b_2$ and $3a_1$ of Al_3 ($^4A_2$) localized in the Al_3 plane, respectively. The small spin density (0.04) on the Na atom suggests that both SOMO's are mostly localized on Al_3. The bond distances R_{Al-Al} is shortened substantially from those of the parent Al_3. A Na atom is bonded to one of Al atoms more strongly than to the other two.

The stable singlet state is the $^1A_1'$ of a tetrahedral form with C_{3v} symmetry, and its electron configuration has a closed shell as

$$^1A_1'[(1a_1')^2(1e)^4(2a_1')^2(3a_1')^2]\ (C_{3v})\ (\mathbf{3a}),$$

and this state is probably the ground state of Al_3Na. Because the energy difference between $^3A''$ and $^1A_1$ is 0.43 eV, more accurate calculations with the electron correlation may change the state ordering, as in Al_2Na. This state is formed by adding a Na atom above the center of the equilateral triangular Al_3 ($^2A_2''$). Again, the shortening of R_{Al-Al} from 2.85 Å in Al_3 ($^2A_2''$) to 2.72 Å in Al_3Na is seen. The parentage of the orbital $2a_1'$ is $3s_{Na}$ and $1a_2'$ of Al_3 ($^2A_2''$), and this orbital is the bonding

orbital between Al_3 and a Na atom. The positive charge on Na is smaller than in the $^3A''$ state. In general, with a few exception, the positive charge on a Na atom in the state with lower multiplicity is smaller than in the state with higher multiplicity.

The removal of an electron from 2a″ of the $^3A''$ state and from 3a′ of the $^1A'$ state produces the cationic state $^2A'$ $[(1a')^2(1a'')^2(2a')^2(3a')^2(4a')^1]$ (C_s) (**3d**), which has a deformed tetrahedral form with C_s symmetry. The small spin density of the Na atom shows that SOMO 4a′ is localized on Al_3. But the change of the bond distances R_{Al-Na} as well as R_{Al-Al} is substantial. The positive charge on the Na atom increases by 0.27 from the $^3A''$ state and by 0.40 from the $^1A'$ state. These facts indicate that the orbital reorganization after ionization in the doubly occupied orbitals is large. In a tetrahedral form the $^4A''$ state, whose electron configuration is

$$^4A''[(1a')^2(1a'')^2(2a')^2(4a')^1(2a'')^1(3a')^1]\ (C_s)\ (\mathbf{3e}),$$

is more stable than $^2A'$ state in our approximation. This electron configuration is formed by an electron removal from the doubly occupied 3a′ orbital of the $^3A''$ at the geometry optimization. The geometry of this state is different from that of the corresponding neutral $^3A''$ state drastically Nearly two thirds of spin density are on the Al atom bonded to a Na atom, and the other two Al atoms share the left density; there is almost no spin density on Na atom. The three SOMOs are localized on Al atoms.

In the planar Al_3Na clusters examined, only the $^1A_1$ state of the vertex approach is at a local minimum. The total energy of this state is higher than the sum of the total energy of $Al_3(^4A_2)$ and $Na(^2S)$ in the RHF approximation. Nevertheless, all of the eigenvalues of the force constant matrix are positive. The higher level of approximation with electron correlation might make this state more stable than Al_3+Na. This electron configuration is

$$^1A_1[(1a_1)^2(2a_1)^2(1b_1)^2(3a_1)^2(1b_2)^2]\ (C_{2v})\ (\mathbf{3c}).$$

The two orbitals, $2a_1$ and $3a_1$, have the Al–Na bonding nature; in the orbital $2a_1$, $3s_{Al}$, and $3s_{Na}$ and in the orbital $3a_1$, $3p_{Z_{Al}}$, and $3s_{Na}$. The equilateral bond length in the mixed cluster becomes longer than the other Al–Al bond, while in the Al_3 the equilateral bond is shorter than the other one. The charge on the Na and the neighboring vertex Al atom indicate the ionic bond between the two atoms.

In the in-plane vertex C_{2v} approach two examined triplet states, $^3B_2$ and $^3A_1$, are transition states because the imaginary harmonic frequencies, 82.67i, and 1134.94i and 14.79i cm^{-1}, respectively, are found. These electron configurations are

$$^3B_2[(1a_1)^2(2a_1)^2(1b_1)^2(3a_1)^2(1b_2)^1(4a_1)^1]\ (C_{2v})$$

and

$$^3A_1[(1a_1)^2(2a_1)^2(1b_1)^2(1b_2)^2(3a_1)^1(4a_1)^1]\ (C_{2v}).$$

On the other hand, in the side approach of a Na atom, all of the examined states are transition states. The imaginary harmonic frequencies, 47.48i ($^1A_1$), 160.04i and 64.74i ($^3A_2$), and 153.49i and 24.65i cm^{-1} ($^3B_1$) are obtained with the vibration analysis. These electron configurations are

$$^1A_1[(1a_1)^2(2a_1)^2(1b_1)^2(3a_1)^2(1b_2)^2]\ (C_{2v})$$
$$^3A_2[(1a_1)^2(2a_1)^2(1b_1)^2(3a_1)^2(1b_2)^1(2b_1)^1]\ (C_{2v})$$
$$^3B_1[(1a_1)^2(2a_1)^2(1b_1)^2(3a_1)^2(4a_1)^1(2b_1)^1]\ (C_{2v})$$

The removal of an electron from the $1b_2$ of $^1A_1$ in the in-plane vertex approach produces the cationic state $^2B_2$ (**3f**). The three Al–Al lengths of this state become longer than those of neutral state $^1A_1$. An unpaired electron is localized on Al_3, while the charge on Na of $^2B_2$ increases by 0.32 with ionization. In this paper the cationic quartet state of the in-plane vertex approach is not examined because the triplet states of the neutral Al_3Na are all transition state though we have obtained the stationary geometries.

Geometries of the Neutral and Cationic Al_4Na Clusters. To optimize the geometry of the mixed cluster Al_4Na, we examine the out-of-plane and in-plane vertex approaches to a rhombus Al_4. The approach to a side of rhombus Al_4 is also examined, but the stable structure cannot be obtained. In both out-of-plane and in-plane approaches, the stable doublet and quartet states are found. Similarly to the smaller clusters, the states with higher multiplicity are slightly more stable in the present calculation than with lower multiplicity. But, in reality the doublet states are most probably lower than the quartet state in each conformer.

The quartet state in the out-of-plane approach keeps the rhombus shape unchanged, and has C_{2v} symmetry. The electron configuration is the $^4B_2$ $[(1a_1)^2(1b_1)^2(1b_2)^2(2a_1)^2(3a_1)^2(1a_2)^1(2b_1)^1(4a_1)^1]$ (C_{2v}) (**4b**) of a deformed pentahedral form. This structure is confirmed to be stable by evaluating the eigenvalues of the force constant matrix. Both diagonal and side Al–Al bond distances are shortened by a adsorbed Na atom. The parentage of the doubly occupied orbital $3a_1$ is the lowest unoccupied molecular orbital (LUMO), $1b_{3u}$, of the $Al_4(^3B_{1u})$ and $3s_{Na}$. The parentage of the orbital $1a_2$ is $1b_{3g}$, which is highest doubly occupied molecular orbital of the $Al_4(^3B_{1u})$. In the adsorption of a Na on Al_4 it is noted that an electron transfers from $1a_2$ to $3a_1$ of the Al_4Na (from $1b_{3g}$ to $1b_{3u}$ of the Al_4). It suggests that this state becomes stable by the occupation of the out-of-plane orbital. The small spin density on Na indicates that the electrons of SOMO is localized on the in-plane orbitals of the Al_4. By removing an electron from the highest SOMO $4a_1$ of the $^4B_2$ state, the $^3B_2$ cation is obtained. The optimized structure has not a rhombus Al_4, and the state becomes $^3A''$ (**4f**). The stability of this structure is confirmed. The energy difference from the state having C_{2v} symmetry is only 0.014 eV, although the geometrical structure is appar-

ently changed drastically.

The stable doublet state in the out-of-plane approach is the $^2A'$ (**4a**) state of a distorted pentahedral form with C_s symmetry. At first, we have found the stationary geometry of the $^2A_1$ state, but one eigenvalue of the force constant matrix is negative ($110.82i$ cm^{-1}). The more stable $^2A'$ state has been found by breaking the symmetry, and no imaginary harmonic frequencies are found at the stationary geometry. The energy of this state is very close to the above transition state $^2A_1$. The electron configuration is

$$^2A'[(1a')^2(1a'')^2(2a')^2(3a')^2(4a')^2(2a'')^2(5a')^1]\ (C_s).$$

This structure has the Al_4 and the Al_2Na planes. The Al_4 part does not keep the rhombus shape, and in the Al_2Na plane two Al–Na bonds are not equivalent; the bond distances are 3.324 and 3.311 Å. The orbitals 4a′ and 5a′ have the Al–Na bonding nature, as the orbitals $3a_1$ and $4a_1$ of the $^4B_2$ state have. The large spin density (0.39 and 0.46) on two Al atoms, whose the charge is negative, suggests that an electron of the orbital 5a′ is localized on these Al atoms on the Al_4 plane.

The removal of an electron from the orbital 5a′ in the $^2A'$ state produces the $^1A'$ ionic state, but the state is more stable at C_{2v} symmetry and becomes the $^1A_1$ ionic state (**4e**). The stability of the structure is confirmed by the harmonic frequency analysis. The rhombus structure of the ion changes from that of the neutral cluster, and the bond distance of Al–Na becomes longer. As the spin density of the neutral suggests, the SOMO 5a′ is mostly localized on Al_4, but the charge on Na in the ionic $^1A_1$ state increases by 0.23 with a removal of an electron from 5a′.

In the in-plane vertex approach for each multiplicity, the $^2A'[(1a')^2(1a'')^2(2a')^2(3a')^2(2a'')^2(4a')^2(5a')^1]$ (C_s) (**4c**) of the plane type and the $^4A''$ $[(1a')^2(2a')^2(1a'')^2(3a')^2(4a')^2(2a'')^1(5a')^1(6a')^1]$ (C_s) (**4d**) of the zig-zag type are optimized. In these states the eigenvalues of the force constant matrix are positive. In the vertex $^2A'$ state (**4c**) all Al and Na atoms lie on the same plane. The Al–Al distances are shorter than those of the parentage $Al_4(^3B_{1u})$. The cationic $^1A'$ state (**4g**) is formed by the ionization of this state. The cationic state is also planer. Both diagonal and side Al–Al bonds become longer by the ionization of the $^2A'$ state. The orbital 5a′, from which an electron is removed, of the $^2A'$ state has the Al–Al bonding nature.

In the $^4A''$ state (**4d**) the Al_4 part is bending: dihedral angle is 105.1°, and the Na–Al–Al angle shows 130.1°. Both diagonal and side Al–Al bond distances are shortened by a Na atom adsorbed. The small spin density on a Na indicates that three electrons of unoccupied orbitals are localized on Al_4. The removal of an electron from the orbital 6a′ produces the cationic $^3A''[(1a')^2(2a')^2(1a'')^2(3a')^2(4a')^2(5a')^1(2a'')^1]$ (C_s) (**4i**) state. The side Al–Al distances are shortened by the ionization though the diagonal Al–Al length are slightly longer than that of the neutral $^4A''$ state.

Table 4. Vertical and Adiabatic Ionization Energies of Al_nNa (n=1—4) Clusters

	State	Vertical/eV	Adiabatic/eV
AlNa	$^1\Sigma^+\rightarrow{}^2\Sigma^+$	4.061*[a]	4.043
	$^3\Sigma^-\rightarrow{}^2\Pi$	4.393	4.164
	$^3\Pi\rightarrow{}^2\Sigma^+$	4.286	4.267
MRSD-CI	$^1\Sigma^+\rightarrow{}^2\Sigma^+$	4.813*	4.798
	$^3\Sigma^-\rightarrow{}^2\Pi$	4.673	4.449
	$^3\Pi\rightarrow{}^2\Sigma^+$	4.634	4.543
Al_2Na (Triangular)	$^2A_1\rightarrow{}^3A'$	4.606*	4.469
	$^2A_1\rightarrow{}^1A_1$	5.017	4.988
	$^4B_2\rightarrow{}^3A'$	5.185	4.704
(Linear)	$^2\Pi\rightarrow{}^1\Sigma^+$	4.311	4.102
	$^2\Pi\rightarrow{}^3\Pi$	4.325	4.294
	$^4\Sigma^-\rightarrow{}^3\Pi$	4.707	4.500
Al_3Na (Tetrahedral)	$^1A_1'\rightarrow{}^2A'$	4.732*	4.656
	$^3A''\rightarrow{}^2A'$	5.186	5.087
	$^3A''\rightarrow{}^4A''$	4.464	4.447
(Vertex)	$^1A_1\rightarrow{}^2B_2$	4.437	4.263
Al_4Na (Pentahedral)	$^2A'\rightarrow{}^1A_1$	5.186*	5.123
	$^4B_2\rightarrow{}^3A''$	5.362	5.133
(Vertex)	$^2A'\rightarrow{}^1A'$	4.802	4.638
	$^4A''\rightarrow{}^3A''$	4.879	4.729

a) The value marked is vertical ionization energy from most possible ground state.

Ionization Energy of Al_nNa Clusters. In Table 4 the calculated ionization energy from the stable states of the mixed clusters are summarized. The most possible ground state of the clusters are marked in the table. In the table, the vertical ionization energy implies that the energy is evaluated at the geometry of the neutral cluster, while the adiabatic energy is the energy difference between the neutral and cation clusters, whose geometry is optimized for each state, where the geometry of the cation has the same frame structure with the corresponding neutral cluster. Experimentally the ionization energy is determined by measuring the appearance photon energy, which is, in the photoelectron spectroscopy for simple molecules, the adiabatic energy difference of the neutral and cation system. But, if the geometrical change by ionization is so large, because of less favorable Franck–Condon factors, the adiabatic energy difference cannot be determined by the appearance photon energy. Thus, care must be taken of when the calculated energy is compared with the experimental energy. Since in our definition for the calculated adiabatic energy the geometries of the neutral and cation clusters are similar to each other, though not identical, two energies does not much differ from each other, as Table 4 shows. Because of the definition, the adiabatic ionization energy is slightly smaller than the vertical one. In the table the energies of some of the possible initial states are given. The calculated energies are dependent on the multiplicity, the proper assignment to the ground state of the cluster is required for comparison of the ionization energy with experiments.

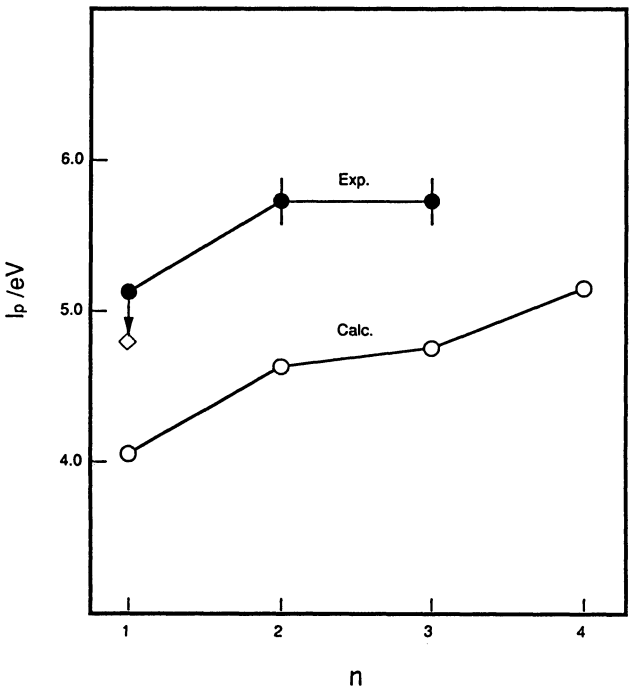

Fig. 4. Calculated and experimental vertical ionization energies of Al_nNa (n=1—4) cluster with the number of Al (n). The experimental energies with error bar are those of Nakajima et al.[5] ○: SCF calculation, ●: Experimental, ◇: CI calculation.

Figure 4 compares the experimental and calculated ionization energy, where the calculated energy is for the most possible ground state of the clusters with lower multiplicity. The experimental energies are those of Nakajima et al.[5] In the figure, the MR SDCI energy for AlNa (4.81 eV) is shown, and it is in good agreement with the experimental energy (<5.15 eV). It is known that the ΔSCF method for the ionization energy generally underestimates the experimental value, because the cation has less electrons and thus the electron correlation is less important than the corresponding neutral system. The calculated n dependence up to n=3 agrees with the experimental one, as seen in Fig. 4; the ionization energy increases with the size of the parent Al cluster. In this plot, we assumed that the ground state of Al_2Na is $^2A_1$, not linear $^2\Pi$, though the energy difference is very small (0.048 eV): if the latter is assumed to be the ground state, the correlation with the experimental plot becomes worse.

As was repeatedly mentioned, the ionized orbitals are mostly localized on the Al part except for the diatomic molecule. Nevertheless, the increase of the positive charge on a Na atom is well correlated with the calculated ionization energy; a large increase of the positive charge reduces the ionization energy. This implies that not the nature of the ionized orbital but the orbital reorganization after ionization is responsible for the reduction of the ionization. This is one of the most important findings in the present study.

Conclusion

The geometries of the most stable and low-lying states in the neutral and cationic Al_nNa (n=1—4) clusters have been optimized at the RHF level of approximation with 6—31 G basis set. In the ground state of both Al_nNa and Al_nNa^+ the frame of the parent Al cluster is kept unchanged, but the shortening of R_{Al-Al} is found in most of the mixed clusters. The out-of-plane π orbital in both Al_n and Al_nNa clusters plays an important role for the shortening R_{Al-Al}. In the neutral mixed clusters with an open shell, the spin density on a Na atom is smaller than 0.1 except for the $^4B_2$ state of Al_2Na. The gross charge of Na in the neutral clusters is less than 0.5 in most states, which implies that the electron-transfer to the Al cluster from a Na atom is only partial. The ground state of the cation is produced by an electron removal from the mostly Al orbital, but the orbital reorganization after the ionization is large: hence the positive charge on the Na atom increases.

The vertical ionization energy of Al_nNa increases with the number of the Al atom. It agrees with the experimental result, qualitatively.

By the examination of the molecular orbital on the Al_2Na it is found that the Al–Na bond is three-center-two-electron bond, and that $3p_z$ function of Na is as important as 3s functions of Na in the bonds. The three-center two-electron bond in Al_2Na is different from that in diborane because the orbital $2a_1$ which form the three-center two-electron bond, also contributes to shortening the Al–Al bond.

The authors are sincerely grateful to Professor Koji Kaya, Dr. Atsushi Nakajima, and Mr. Kuniyoshi Hoshino in our department for their informative discussion.

References

1) H. P. Bonzel, *Surf. Sci. Rep.*, **8**, 43 (1987).
2) "Physics and Chemistry of Alkali Adsorption," ed by H. P. Bonzel and G. Ertl, Elsevier, Amsterdam (1989).
3) W. D. Farley and A. W. Castleman, Jr., *J. Chem. Phys.*, **92**, 1790 (1990).
4) V. Bonačić-Koutecký, P. Fantucci, and J. Koutecký, *Chem. Phys. Lett.*, **166**, 32 (1990).
5) A. Nakajima, K. Hoshino, T. Naganuma, Y. Sone, and K. Kaya, *J. Chem. Phys.*, **95**, 7061 (1991).
6) T. Hanawa, H. Matsuzawa, K. Suzuki, and S. Iwata, to be published.
7) L. G. M. Pettersson and C. W. Bauschlicher, Jr., *J. Chem. Phys.*, **87**, 2205 (1987).
8) T. H. Upton, *J. Chem. Phys.*, **86**, 7054 (1987).
9) M. W. Schmidt, K. K. Baldridge, J. A. Boatz, J. H. Jensen, S. Koseki, M. S. Gordon, K. A. Nguyen, T. L. Windus, and S. T. Elbert, *QCPE Bulletin*, **10**, 52 (1990), *GAMESS*, NDSU version.
10) M. Dupuis, D. Spangler, and J. J. Wendoloski, "NRCC Software Catalog," Vol. 1, program No. QG01, *GAMESS* (1980).

11) M. J. Frisch, M. Head-Gordon, H. B. Schlegel, K. Raghavachari, J. S. Binkley, C. Gonzalez, D. J. Defrees, D. J. Fox, R. A. Whiteside, R. Seeger, C. F. Melius, J. Baker, R. L. Martin, L. R. Kahn, J. J. P. Stewart, E. M. Fluder, S. Topiol, and J. A. Pople, GAUSSIAN 88, Gaussian, Inc., Pittsburgh PA, USA (1988).
12) W. Pewestorf, V. Bonačić-Koutecký, and J. Koutecký, *J. Chem. Phys.*, **89**, 5794 (1988).
13) Z. Fu, G. W. Lemire, G. A. Bishea, and M. D. Morse, *J. Chem. Phys.*, **93**, 8420 (1990).
14) W. R. M. Graham and W. Weltner, Jr., *J. Chem. Phys.*, **65**, 1516 (1976).
15) C. W. Bauschlicher, Jr. and L. G. M. Pettersson, *J. Chem. Phys.*, **87**, 2198 (1987).
16) M. F. Cai, T. P. Dzugan, and V. E. Bondybei, *Chem. Phys. Lett.*, **155**, 430 (1989).
17) Y. M. Hamrick, R. J. Van Zee, and W. Weltner, Jr., *J. Chem. Phys.*, **96**, 1767 (1992).
18) S. Iwata, S. Saeki, T. Naganuma, T. Hanawa, H. Matsuzawa, K. Suzuki, A. Nakajima, and K. Kaya, to be published.